

Antenna Using a Magnetic-Slab Located in the Principal Magnetic-Field Region beneath the Patch

Ignacio J. Garcia Zuazola^{1, *}, Ashwani Sharma², Misha Filip¹, and William G. Whittow³

Abstract—This paper presents an analysis of microstrip patch antennas with different dielectric/magnetic substrate profiles in an attempt to obtain operating frequency reduction. Initially, different ridge shapes in the substrate were examined. An in-depth investigation of the ridge shape and its dimensions on the antenna performance has been carried out. Subsequently an antenna with a magnetic-slab loaded in the prime magnetic-field region beneath the patch is proposed. The new magnetic loaded antenna design is aimed to reduce the resonant frequency of a conventional patch and reduce the profile of an earlier design with a substrate ridge. Various magnetic materials have been embedded within the original dielectric substrate of the patch antenna. Measured results validated the hypothesis that this frequency can be reduced by placing magnetic materials at the centre of the patch. The achieved gain is expected to be further enhanced by using forthcoming magnetic materials with improved performance.

1. INTRODUCTION

Materials and metamaterials have been used as parasitic components for antenna miniaturization, and a resistive or reactive loading technique is common for this purpose [1]. Pure dielectric, magnetic, and magneto-dielectric materials beneath patch antennas are encountered in the literature for mitigating the impact of reflections between the radiating source and its image currents due to ground planes that lead to reduced antenna efficiency and bandwidth (BW); the use of a reactive material is well known to minimize this effect. Among common magnetic materials, the ferromagnetic, typically iron, cobalt, and nickel are conductive and therefore not beneficial in this antenna setting; the ferrimagnetic, enriched magnetic ordering exhibits magnetization as well as dielectric properties [1,2]. Among magneto-dielectric materials, a current trend is attributed to ferrites due to their inherent relative high insulation and permeability at low frequencies, typically below 300 MHz. However, there is no literature evidence of ferrites used in specific regions where the antenna's dielectric properties are minimal, despite the Snoek operating frequency f_o limit of ferrites [3]. In this paper, embedding magnetic materials in certain locations is preferred over making the whole substrate magnetic in terms of material usage. Fundamentally, high permittivity ϵ leads to narrow BW with narrower fringing fields that lead to poor radiation and lower ϵ circumvents concentrations of electric field (E -field) in the permittivity region. High permeability μ typically broadens the BW; the efficiency of the antenna is predominantly constrained by electric and magnetic losses [4] in the substrate. Since the E -field at the centre of an antenna's patch along its non-radiating edges approximates to zero, ϵ is not deemed crucial. This is because at the centre of the patch (where the prime magnetic-field (H -field) region occurs) the relative permittivity ϵ_r has little effect on the dielectric loading as the E -fields are small here.

Received 3 January 2021, Accepted 24 February 2021, Scheduled 8 March 2021

* Corresponding author: Ignacio J. Garcia Zuazola (ignacio.garcia-zuazola@port.ac.uk).

¹ Faculty of Technology, University of Portsmouth, Portsmouth, Hampshire PO1 3DJ, UK. ² Electrical Engineering Department, Indian Institute of Technology Ropar, Punjab, India. ³ Wolfson School of Mechanical, Electrical and Manufacturing Engineering, Loughborough University, Loughborough, Leicestershire, LE11 3TU, UK.

A ε_r loading near the edges of the patch down-shifts f_r at the expense of a lowered antenna radiation efficiency [4]. On the contrary, increasing relative permeability μ_r in this local H -field region leads to a better effect as the H -fields are larger here. It contributes to lowering f_r with moderate impact on losses and stored energy [1] and counterbalances the poor efficiency and BW originated by ε_r [5]; this is feasible as a 3-dimensional (3D) shape of the substrate at the centre of the patch was found insensitive to ε_r [6]. Any 3D shape however increases the height of the antenna in the z -axis. The f_r down-shift factor is defined by the refractive index n of electromagnetic radiation, next.

$$n = \sqrt{\varepsilon_r \mu_r} \quad (1)$$

where ε_r is the material's relative permittivity and μ_r its relative permeability.

f_r is well-known given as,

$$f_r \approx \frac{c}{2ln} \quad (2)$$

where c is the velocity of light and l the length of the patch.

From Eq. (2) the patch antenna's width w has no effect on f_r as it controls the impedance Z and radiation pattern of the antenna [4]. Material losses are inherent and given by the dissipating factor D which is inversely proportional to the quality factor Q [1], such that

$$\tan \delta_\mu = \mu''/\mu' = D_\mu = 1/Q_\mu \text{ and } \tan \delta_\varepsilon = \varepsilon''/\varepsilon' = D_\varepsilon = 1/Q_\varepsilon. \quad (3)$$

A f_r down-shift is given by n , $Z/Z_o \approx 1$ (Z_o is the impedance of free space), and the admissible $\tan \delta_{total} (\tan \delta_\varepsilon + \tan \delta_\mu) \leq 0.1$ [7].

Because of the insensitivity to ε_r in the H -field region, $\tan \delta_\varepsilon$ can be in principle ignored; this allows using bulk ferrites in this region for the microwave spectrum. n is consequently determined by μ_r which, in essence, is the magnetisable degree of a material to a magnetic response. The first magnetic material in literature, the loadstone (Fe_3O_4) data from 400BC to more recent ferromagnetic MK steel, KS steel, Alnico 5 and Nickel; ferrimagnetic cobalt magnets, SmCO_5 , Sm_2Co_5 , $\text{Sm}_2\text{Co}_{17}$ and Neodymium magnets, NdFeB, have prices that are higher for the latest and lowest for magneto-dielectric bulk ferrites. These ferrites possess insulating magnetic oxides with high electrical resistivity, low eddy current and dielectric losses, high μ , and moderate ε [8]. High ε_r leads to higher conductance and to more H -field lines (flux) concentrations in the prime H -field region beneath the patch; it is to alleviate these flux concentrations of why bulk ferrites are preferred due to their highest μ . Among ferrites, spinel MFe_2O_4 , where $\text{M} \rightarrow \text{Co}, \text{Ni}, \text{Zn}, \text{ and } \text{Cd}$, are common and relatively inexpensive; garnet $\text{R}_3\text{Fe}_5\text{O}_{12}$, where $\text{R} \rightarrow \text{Yttrium}$ and magneto-plumbite hexaferrites $\text{MFe}_{12}\text{O}_{19}$, where $\text{M} \rightarrow \text{Ba}, \text{Sr}, \text{ and } \text{Ca}$, are more expensive but widely used in permanent magnets with high magnetic coercivity. Advantages in the use of magnetic materials have been reported in [3] and [9]; however, this paper is not intended to overcome other typical conventional miniaturization methods. Ferrite sheet loading for antenna miniaturisation, for instance, has been reported in [10–13] with a f_r down-shift of $\sim 70\%$ at 900 MHz and $\sim 6\%$ at 1.72 GHz without compromising performance. Here, several magnetic materials are embedded within the original dielectric substrate of the antenna in the prime H -field region beneath the patch for potential frequency reduction; this is realizable providing that they possess a high μ and low $\tan \delta_\mu$ at resonance to effectively strengthen the flux density of the H -field at the centre of the patch.

2. DESIGN OF ANTENNA WITH MAGNETIC-SLAB

An antenna with a magnetic-slab embedded within the original dielectric substrate of the antenna in the prime H -field region beneath the patch is presented. ISM band is defined by the ITU-R 2.4–2.5 GHz (100 MHz BW) worldwide which also covers the FCC 2.4–2.4835 GHz (83.5 MHz BW); although the magnetic loaded antenna resonated at 2.34 GHz it can in principle be tuned for this band. The magnetic loaded antenna is compared to a conventional patch antenna of same dimensions resonating at ~ 3 GHz. Conventionally, microstrip patch antennas are uniformly flat and increasing the substrate height (a ridge) in specific locations where E -fields are small and currents large reduces the frequency [6]. In this work, an earlier design [6] is used and the evolution to the embedded magnetic-slab antenna presented. Consequently, different ridge geometries and magnetic-slab loadings are studied. Fig. 1(a)

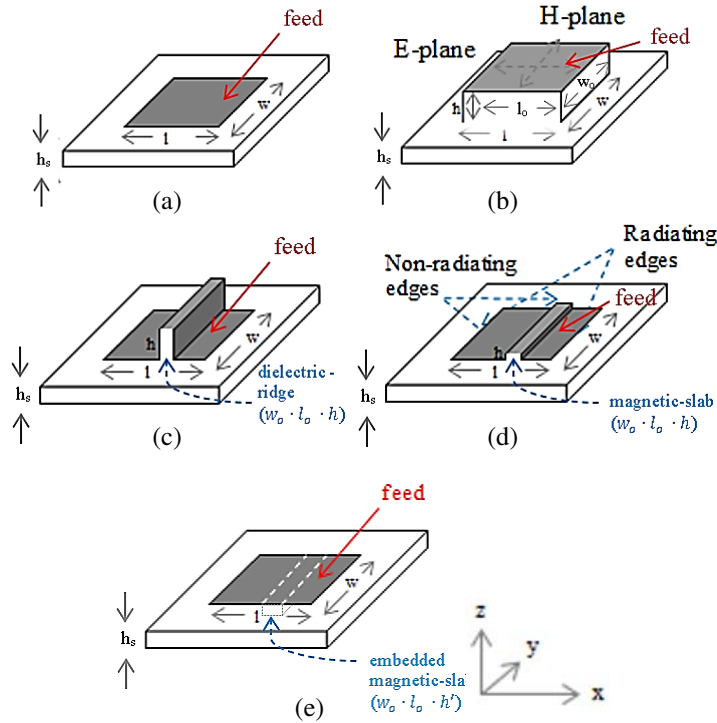


Figure 1. Design evolution of the antenna, (a) the conventional patch antenna, (b) with thicker substrate, (c) with a dielectric ridge, (d) with decreased h using magnetic-slab, and (e) with embedded magnetic-slab.

shows the conventional patch antenna, design a; Fig. 1(b) a modified version using a thicker dielectric substrate, design b; Fig. 1(c) a modified version with a dielectric ridge as reported in [6], design c; Fig. 1(d) a modified version with decreased height h using magnetic-slab, design d; and Fig. 1(e) the evolved design with a magnetic-slab embedded within the original dielectric substrate of the antenna in the prime H -field region beneath the patch, design e. All designs were fabricated using a substrate (Taconic) of thickness, $h_s = 0.8$ mm, $\epsilon_r = 2.2$ and $\tan \delta_E = 0.0009$ on a 70×70 mm ground plane with a patch radiator of 30×32 mm (w, l) and fed using an SMA connector through a via from the ground plane at coordinates $w = 15$ and $l = 12$. The total height of the antenna, h_T , was amendable and had a highest h given by $h_T (h + h_s) = 2.4$ mm, where h is the height of the increased substrate in the z -axis and h_s the original substrate thickness.

Design a was used to determine the initial f_r of a conventional patch antenna with a geometry shown in Fig. 1(a) and design parameters as immediately outlined.

Design b is an extended version of design a using a thicker substrate set beneath the patch ($h = 1.7$ mm \rightarrow $h_T = 2.4$ mm) and shown in Fig. 1(b). This design is introduced as a base for consecutive designs. The thicker substrate widens the antenna's BW with unnoticeable f_r difference. Although this BW increase is widely known [4], this design is reported for comparison purposes. Therefore, a higher h increases the BW response, and a lower h makes Z of the antenna become less inductive [14]. Increased BW using non-planar substrates has been reported in [15]. However, increasing h only in the prime H -field region beneath the patch is an alternative approach to frequency reduction; the revised design is introduced subsequently.

Design c is shown in Fig. 1(c) and is a modified version of design b using that increased h in a specific location of the patch only; this is to build upon solid results and for comparison purpose. Varying the 3D shape of the substrate and metallic patch, the resonant frequency can be reduced [6]. Thus, different ridge shapes (silhouettes) are considered to investigate the effect on the antenna performance when smoothing the flow of the electrical currents along the patch; this is presented in Section 3.

Design d is shown in Fig. 1(d) and is an extended version of design c using a magnetic-slab instead

of a dielectric ridge. This is loaded to decrease f_r of the antenna using highly magnetic μ materials with the aim to lower h substantially. Various commercially available materials were designated for the study; they are defined next. Ferrite composites from Laird, a) Eccosorb NS1000Series, b) MHLLSeries of $\epsilon_r \approx 595$, $\mu_r \approx 7.13$, and $\tan \delta_E \approx 0.72$, $\tan \delta_M \approx 0.74$ at ~ 2.4 GHz, and NiCo ferrite [3] $\epsilon_r \approx 13$, $\mu_r \approx 10$ and $\tan \delta = 0.05$ at ~ 2.4 GHz; a total of 11 flexible commercially available sheets were assembled for $h \approx 1.7$ mm. Other available materials such as the MnZn bulk ferrite (found in toroids), the NdFeB (strongest permanent magnet found in hard-disk devices), the yttrium iron garnet (YIG), and the BaFe (found in fridge magnets, speaker magnets, floppy disks and recording tapes) were also used in the experimentation; 21 assembled sheets of BaFe floppy tape were needed for $h \approx 1.7$ mm.

Design e is shown in Fig. 1(e) and is a modified version of design d using a magnetic-slab embedded within the original dielectric substrate of the antenna in the prime H -field region beneath the patch. That implied making a slot in the original substrate to embed a magnetic material in its interior of height h' . As a result, design e had seemingly same dimensions as design a with reduced frequency. As with design d, a Laird a) Eccosorb NS1000Series, b) MHLLSeries and a NiCo, with material properties immediately outlined were designated for the study; a total of two flexible commercially available sheets were assembled for $h' = 0.17$ mm. MnZn powder, BaFe (floppy disk recording tapes) and nickel sprayed film were similarly used in the experimentation; two BaFe floppy tapes were assembled for $h' = 0.17$ mm.

3. ANALYSIS AND RESULTS

For the evaluation, the antennas introduced in Section 2 were simulated using CST Microwave Studio and corroborated by measurements. The antenna was simulated using a coaxial feed line designed for a 50Ω characteristic impedance and open boundary conditions for the simulation setup. The simulated material for the ridge in designs a–c used dielectric $\epsilon_r = 2.2$ and $\tan \delta_E = 0.0009$, whereas for the d and e used magnetic $\epsilon_r \approx 13$, $\mu_r \approx 10$ and $\tan \delta = 0.05$ at ~ 2.4 GHz. The designs were measured and compared to simulated results. The reflection coefficient (S_{11}) responses are shown in Fig. 2 (d' denotes design d with initial $h = 1.7$ mm).

As predicted, design a resonated at ~ 3 GHz; design b increased the BW with unnoticeable f_r

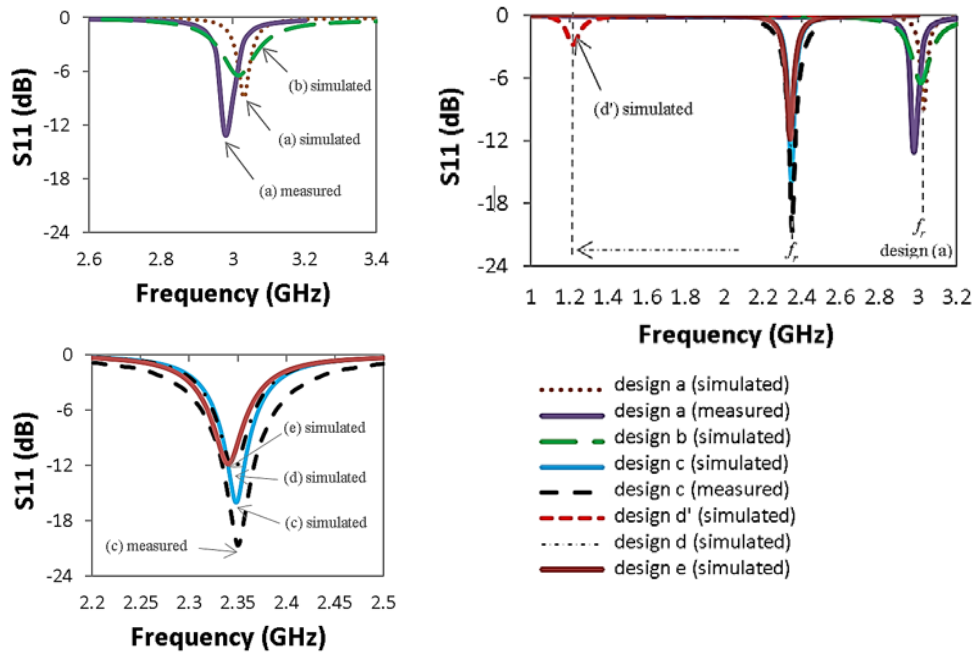


Figure 2. Simulated and measured S_{11} responses of the antenna designs, (top left) over a frequency of 2.6–3.4 GHz, (bottom left) over a frequency of 2.2–2.5 GHz and (right) in wider observation over 1–3.2 GHz.

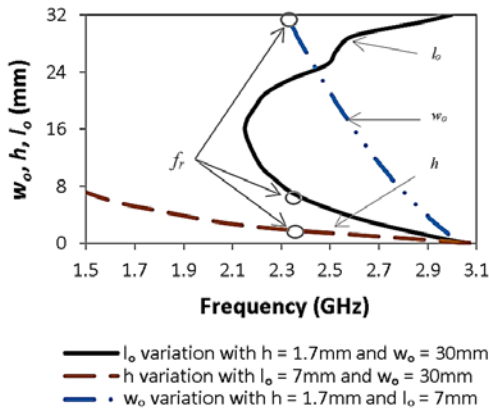


Figure 3. Simulated effect of w_o , l_o , and h on frequency using design b.

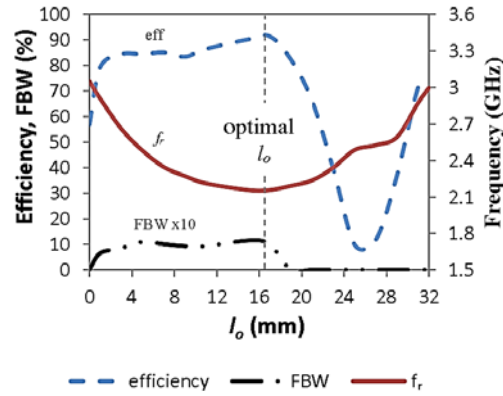


Figure 4. Simulated efficiency, FBW and f_r responses of design evolution from b to c with $\epsilon_r = 2.2$, $h = 1.7$ mm, $w_o = 30$ mm and varied l_o .

difference; and design d' resonated at ~ 1.2 GHz. The responses of designs c–e intentionally resonated at pretty much the same central frequency since the authors strived for miniaturising the antenna in the z -axis (reduced h). Measurements showed reasonable agreement with simulated results. Formerly, the ridge length l_o of design b was shortened equally from both edges along the E -plane (x -axis) since h was in close proximity to the radiating edges of the patch impacted negatively on the antenna's efficiency and allowed f_r tuning, the feed remained at the original coordinates $w = 15$ and $l = 12$. Fig. 3 shows the simulated effect of w_o, l_o and h on frequency using design b and finds the optimal parameter values (w_o, l_o, h) of design c with regards to f_r , w_o shortened equally from both edges along the H -plane (y -axis), and h shortened in the z -axis. It was observed that when $l_o \leq 17$ mm, the frequency of operation was decreased, and on the contrary when $l_o > 17$ mm < 32 mm the frequency of operation was increased. Therefore, the maximum reduction in resonant frequency occurs when $l_o \approx \frac{1}{2} l \approx 17$ mm. This is because for > 17 mm as the ridge l_o approaches the total patch length l , the resonant frequency approaches the value of the unloaded regular patch, design b (Fig. 1(b)); this is ~ 3 GHz (Fig. 2) when $l_o \approx l \approx 32$ mm. It was witnessed that $l_o > 32$ mm contributed to a reduced f_r with compromised efficiency. Compared to when l_o was 17 mm, $l_o = 51$ led to a 31% compromised efficiency and zero BW measured at -10 dB S_{11} and f_r 2.14 GHz. Further observations suggested a rational argument for using $h \approx 1.7$ mm since a lengthened h decreased f_r of the antenna at the expense of a compromised efficiency (i.e., 66.5% for $h = 6.25$ mm), which is a constrained gain of -1 dBi compared to when h was 1.7 mm.

Figure 4 shows the simulated efficiency, fractional bandwidth (FBW), and frequency responses of design evolution from b to c with varied l_o , both efficiency and FBW calculated for the resonance frequency corresponding to a specific length l_o . The optimal l_o is revealed and occurs when higher efficiency, FBW, and reduced f_r were found; this is when $l_o \approx 17$ mm. Therefore, design c (uses $l_o = 17$ mm) resonated at ~ 2.34 GHz with a tuning control of its f_o between 2.12 and 2.43 GHz from a varying l_o , which would allow the antenna to be in-band. Although a wider range f_r control seemed likely, this was constrained by efficiency. l_o was shortened equally from both edges along the E -plane (x -axis) and predictably up to the prime H -field region of the patch.

Moving the resulting ridge towards the radiating edges of the patch is undesirable since it up-shifts the antenna's f_r [6] caused by the relatively higher surface currents of narrowing fringing fields that are present at these edges; therefore, the ridge is kept at the centre of the patch. It was reported in [6] that a ridge placed over the antenna's ground plane led to similar f_r reduction; however, due to the slightly increased f_r observed in a new set of simulations the ridge was kept below the antenna's patch. Fig. 5 shows the simulated efficiency, FBW, and f_r responses of design c with $h = 1.7$ mm and varied ridge's ϵ and μ ; $\tan \delta_E = 0.0009$ and $\tan \delta_M = 0.05$ at ~ 2.34 GHz. The ridge position is shown in Fig. 1(d), which is at $l = 9.5$ mm (in the x -axis direction). f_r remained practically unchanged when ϵ_r varied from ~ 3 to 20; this is in accordance to [6] where a 3D shape of the substrate at the centre of the patch was

insensitive to ε_r . The antenna efficiency degraded for higher ε values, and ε had insignificant effect on the antenna's f_r . In contrast, it can be observed that μ did not deteriorate efficiency, and a higher μ rendered to f_r reduction; a rational argument to use a magnetic-slab instead of a dielectric ridge later on. The fact that the efficiency was preserved when the magnetic constant was increased was due to the varied μ in the patch's ridge and not in the patch's original substrate. The authors next consider different ridge shapes. Results are shown in Table 1.

Table 1. Simulated performance using different.

Shape	Chamfer	f_r (GHz)	RL (dB)	FBW (%)	Peak Gain (dBi)	Peak Efficiency (%)	
soft corners		0°	2.34	16.00	1.02	6.00	85.60
		9°	2.36	16.29	1.03	6.13	86.14
		18°	2.37	16.77	1.03	6.13	86.35
		27°	2.48	21.74	1.03	6.15	87.34
		36°	2.52	25.61	1.02	6.15	87.57
		45°	2.64	27.05	0.95	6.07	87.33
sharp corners		0°	2.34	16.00	1.02	6.00	85.60
		11°	2.39	17.51	1.03	6.13	86.00
		22°	2.39	17.51	1.03	6.14	86.65
		33°	2.50	24.17	1.03	6.14	87.24
		45°	2.64	27.69	0.95	6.07	87.20

These shapes were considered to investigate the effect on the antenna performance when the flow of the electrical currents was smoothed (chamfer) along the patch. The chamfered shapes, however, slightly reduced the electrical length of the antenna compared to that using the initial rectangular shape; therefore, a minor up-shift effect on the antenna's f_r was anticipated. A circumscribed chamfer around the original shape would have the opposite effect at the expense of a bigger antenna volume; a rational argument not to be used in this study.

In conclusion, h controlled f_o of the antenna and was optimal at 1.7 mm (Fig. 3). However, the authors strive for miniaturising the antenna in the z -axis and making it comparable to design a (Fig. 1); therefore, lowering h must be accomplished. It was witnessed that whereas l_o controlled f_r with optimal value 17 mm (Fig. 4), a reduced w_o increased the f_r response of the antenna (Fig. 3); since this is an undesirable effect, w_o was kept at 30 mm. In addition, unlike ε , increasing μ rendered to f_r reduction without compromising the antenna performance (Fig. 5). Concluding remarks suggest the use of magnetic materials instead of dielectrics in this prime H -field region beneath the patch. Whereas magnetization can allow changes in the induced H -field moments, demagnetization leads to the elimination of unwanted H -fields; therefore, to exploit the benefits of potential constructive changes in the E -field due to these changes, a magnetic-slab ($w_o \cdot l_o \cdot h'$) is used and its effect on the antenna's performance studied subsequently. w_o and l_o of the magnetic-slab are consequent from the results in Table 1.

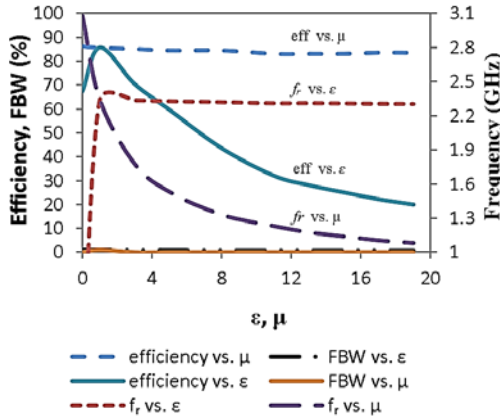


Figure 5. Simulated efficiency, FBW and f_r responses of design c with $h = 1.7$ mm, $l_o = 17$ mm and varied ridge's ϵ and μ .

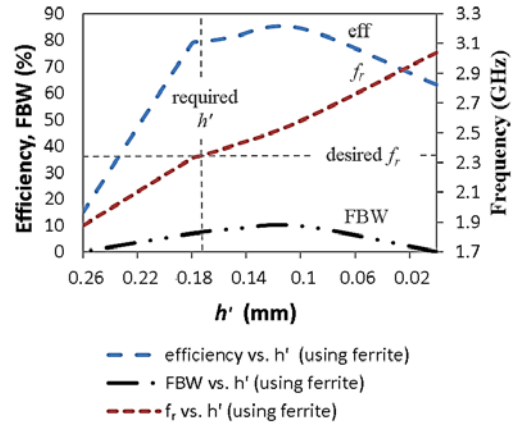


Figure 6. Simulated efficiency, FBW, and f_r responses of design evolution from d to e with $\mu_r = 10$, $\epsilon_r = 13$, $w_o = 30$ mm, $l_o = 7$ mm and varied h' .

3.1. Using Magnetic-Slabs

f_r of an antenna for a given l is dependent on n ; however, it was evidenced that unlike μ_r , high ϵ_r in the local H -field region of the patch compromised the antenna's efficiency with insignificant effect on its f_r ; the use of high μ_r allowed for f_r down-shift without degrading its efficiency. Hence, the use of materials with (ideally) high μ low ϵ is attractive for frequency reduction. Typically, the antenna's H -field (using magnetic material) is intensified for $\mu_r > 1$, even though the E -field inside materials with $\epsilon_r > 1$ is diminished. We therefore strive for magnetic materials with (realistically) high μ_r and moderately low ϵ_r .

The simulated efficiency, FBW, and f_r responses of design evolution from d to e with $w_o = 30$ mm, $l_o = 7$ mm and varied h' are shown in Fig. 6.

For the simulation, a ferrite material with properties $\mu_r = 10$, $\epsilon_r = 13$ found in [13] and $\tan \delta = 0.05$ at 2.34 GHz were used. Results show the required h' to preserve f_o of the antenna at the desired $f_r = 2.34$ GHz. Because ϵ_r and corresponding δ_ϵ are existent in magnetic materials, a trade-off between frequency reduction and efficiency was present. Although there was a margin for improving the efficiency and FBW of the antenna by 1.9% and 2.16% respectively with varied h' , it was at the expense of an increased f_r (by 0.23 GHz). The required h' meant that it went 0.17 mm down the original dielectric substrate of the antenna, which resulted in a magnetic-slab with dimension $w_o = 30$ mm, $l_o = 7$ mm, and $h' = 0.17$ mm for embedding within the original dielectric substrate of the antenna. An additional study relocated the magnetic-slab above the antenna's radiator and kept original Taconic substrate $h_s = 0.8$ mm and $\epsilon_r = 2.2$. A f_r up-shift of 0.69 GHz was observed with a lower efficiency, FBW, and return loss (RL) of 6.14%, 0.72%, and 2.25 dB, respectively. This corroborated the preferred location of the magnetic-slab to be in the principal H -field region beneath the patch of the antenna and its effectiveness, which is predominantly influenced by ϵ_r , to be insensitive when being located in this designated region. Earlier in Section 1, the f_r down-shift factor was defined by n . With the aim to verify that the frequency reduction was in fact due to μ_r (f_r was reported to be insensitive to ϵ_r), n was maintained constant with varied ϵ_r and μ_r ($\sqrt{\epsilon_r \mu_r} = n = 1.48$) and witnessed that f_r , efficiency, and FBW responses of the antenna were unaffected. Assuming a unity VSWR at the design frequency, the quality factor Q_{total} of an antenna may be expressed in terms of FBW and maximum allowable VSWR as Eq. (4) [4] and the zero-order BW (VSWR = 2) for planar microwave antennas with a magneto-dielectric substrate as Eq. (5) [16].

$$Q_{total} = \frac{VSWR - 1}{FBW_{max} \sqrt{VSWR}} \quad (4)$$

$$BW = \frac{96\sqrt{\mu/\varepsilon}t/\lambda_0}{\sqrt{2}[4 + 17\sqrt{\mu\varepsilon}]} \quad (5)$$

where t is the substrate thickness and λ_0 the length of the f_r .

Q_{total} is a figure-of-merit representing the antenna efficiency. Because Q_{total} can be compromised with increased FBW (4), a higher μ can be used for compensation and in principle maintain the original BW (5). Significant BW improvement using magneto-dielectric antennas results when μ is large and ε is close to one; also, a higher μ reduces f_r [16]. Although ε (at the centre of the patch) was earlier reported not to affect the antenna's response, the effect using very high ε however has not been demonstrated in [6, 14, 16] which might impact negatively lower Q_{total} . Therefore, magnetic materials with relatively high μ and moderately low ε are sought for the magnetic-slab in this antenna design, unfortunately, not found commercially available. Table 2 shows the performance comparison (simulated) of designs a–e. Designs a–c used dielectric (earlier introduced Taconic), and designs d and e used magnetic-slab (ferrite). Whereas designs b–d are progressions to design e, designs a and e are the only antennas comparable regarding their physical dimension. It can be observed that, in accordance to Equation (5), higher ε (i.e., design e) contributed to a reduced FBW. Although this is in principle an indication of improving (higher) Q_{total} , higher VSWR (lower RL) compromised Q_{total} (4); the lower gain and efficiency are shown in Table 2. This is a trade-off for the antenna miniaturization. To validate design e experimentally, several commercially available magnetic materials already introduced in Section 2.4 were used. The measured S_{11} responses for the antennas with different magnetic-slab materials are shown in Fig. 7, which include design d using magnetic materials as part of the evolution process from designs d to e. Selected materials are provided in the figure legend.

Table 2. Simulated performance comparison of designs a–e.

Design	f_r (GHz)	RL (dB)	FBW (%)	Gain (dBi)	Efficiency (%)
a	3.03	9.0	0	4.30	57.0
b	3.01	6.5	0	5.42	73.9
c	2.34	16.0	1.02	6.00	85.6
d	2.34	12.6	0.81	5.76	81.1
e	2.34	11.8	0.72	5.74	79.3

Whereas design d used magnetic-slabs of $w_o = 30$ mm, $l_o = 7$ mm, and $h \approx 1.7$ mm, and design e used $w_o = 30$ mm, $l_o = 7$ mm, and $h' \approx 0.17$ mm. In both designs, the MnZn bulk ferrite presents the highest f_r reduction, f_r of design a and the desired f_r are indicated in the figure for consciousness. Initially, the NedB magnet, commonly known as rare magnet and used in hard-disks, was found to be conductive and as a result f_r of the antenna up-shifted by 233 MHz (undesired effect). The BaFe, found in fridge magnets and floppy disks, had insignificant effect on f_r since both unfortunately contain very thin layers of BaFe depositions over a supporting material. The speaker magnet is naturally robust in BaFe and therefore presented a f_r down-shift of ~ 483 MHz. The YIG crystal and ferrite composite from Laird Inc. series a–c and Toda Inc. presented a similar response with poor matching; $RL \leq 2$ dB. The maximum frequency reduction was achieved with the MnZn bulk ferrite. Yet, the resulting antenna's impedance was detuned with respect to the initial Z_{in} . The sprayed nickel was found to be conductive and of no use. Like design d, the MnZn bulk ferrite presented the highest degree of frequency reduction for design e; however, impedance matching had to be tuned to bring the locum of the antenna to resonance. Lossy μ_r material meant poor formation of H -field, therefore, a poor matching due to the poor degree of magnetization but contributed to a lowered f_r . Electrical loss was not significant to the impedance of the antenna. Due to Eqs. (4) and (5), Z of design e was away from the initially intended

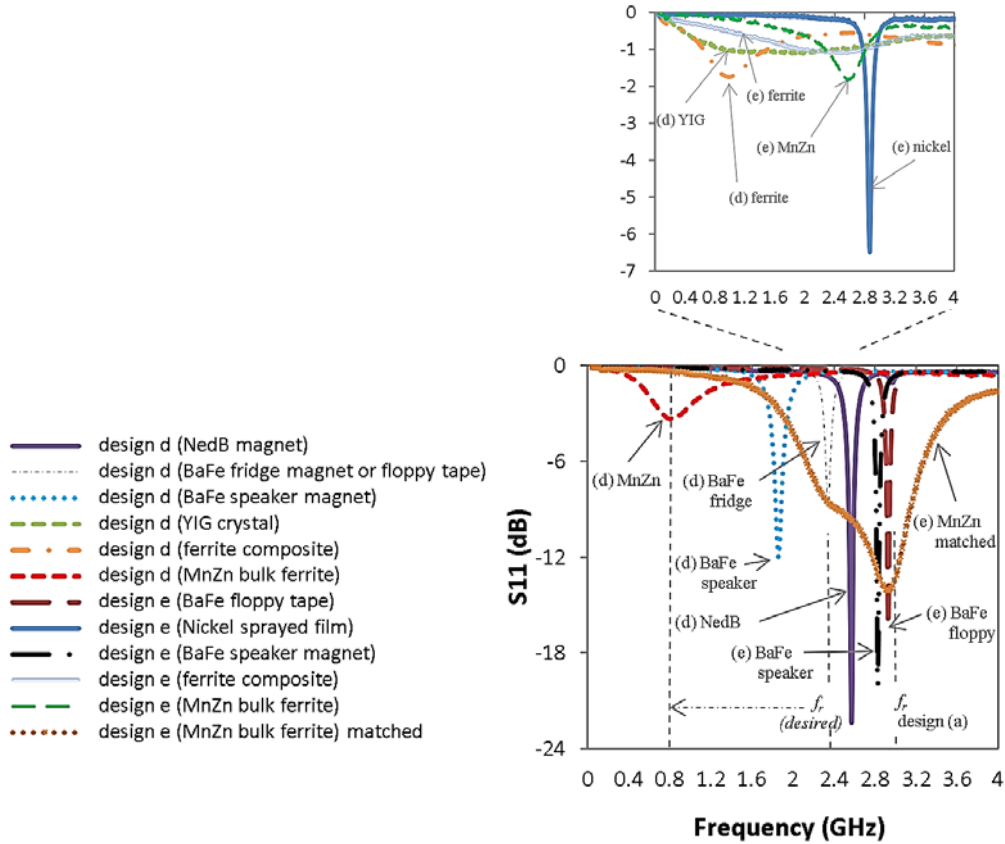


Figure 7. Measured S_{11} of designs d and e with different magnetic-slab materials; the inset (top) shows a closer attention of the figure in greater detail.

matching at 50Ω with $Z \approx 5.423 \Omega$ and led to a demanding matching control (unable to be re-tuned by shortening the radiator’s width w) which mainly attributed to $\epsilon \neq \mu$. A $1/4\lambda$ microstrip matching circuit attached to the feed of the antenna was needed to match the antenna to the intended 50Ω . The response is shown as design e (MnZn bulk ferrite) matched in Fig. 7. Remaining measurements use design e matched. In line with Fig. 6 simulations, the shortened h was intended to bring the frequency response of the antenna back to $f_r = 2.34$ GHz; in the experiments, the optimal $h' \approx 0.17$ mm did not bring the resonance to the desired f_r . The antennas were measured in an anechoic chamber, and the respective radiation patterns of designs a, c, and e are shown in Fig. 8.

Whereas design a was measured at its central frequency of 3 GHz, designs c and e were measured at the desired $f_r = 2.34$ GHz. Note that the frequency reduction for design c is attributed to the increased inductance due to the dielectric-ridge [17, 18] and for design e to the magnetisable degree of the material to a magnetic response due to the magnetic-slab. The patterns are similar for the three designs in the boresight direction (0°) with comparable directivity for designs a and e, but dissimilar patterns in the rear direction (180°) are with slightly greater main backlobes for designs c and e. The measured gain and efficiency of designs a, c, and e are shown in Fig. 9. Design c had a peak realized gain of 5.87 dBi. Although the gains of designs a and e are not comparable since they were meant to resonate at dissimilar frequencies, results show design e with 2.5 dBi and 1.19% inferior gain and efficiency respectively compared to those of design a. This validates design e, which uses an embedded magnetic-slab in the principal H -field region beneath the patch, for f_r reduction with moderate impact on performance; this claim is acceptable since the two antenna designs a and e have the same physical size. Table 3 details the measured performance of designs a, c, and e.

Designs a and e are the only antennas comparable in regard to their physical dimension; design c is included for completeness. Comparison shows a 0.66 GHz f_r down-shift and an increased FBW for design e, and this reaffirms its validation. However, compared to design c, design e was compromised in

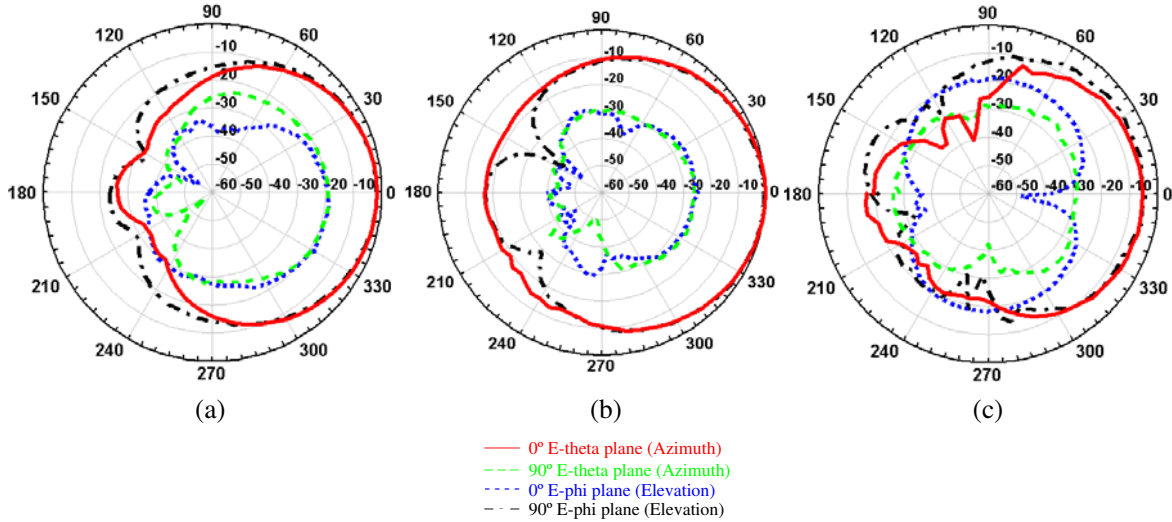


Figure 8. Measured radiation patterns of antennas, (a) design a, (b) design c, (c) design e.

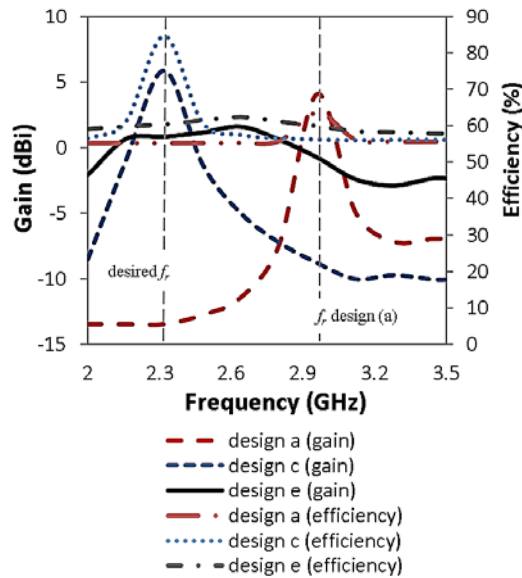


Figure 9. Measured gain and efficiency of designs a, c, and e.

gain and efficiency (by 4.27 dBi and 22.06% respectively) and presented a trade-off for miniaturization at present, but shows potential with the forthcoming use of pending magnetic materials with improved performance.

Using Model 100 harmonics strip-line cavity from Damascus Inc., samples of magnetic materials were measured. Properties of the ferrite composite Eccosorb NS1000Series/MHLLSeries from Laird Inc with respective response $\epsilon_r \approx 595$, $\mu_r \approx 7.13$ and $\tan \delta_E \approx 0.72$, $\tan \delta_M \approx 0.74$ at ~ 2.4 GHz and MnZn bulk ferrite are shown in Fig. 10.

Measurements corroborated the properties of the magnetic materials used in the simulator. However, the commercially available samples are not exclusively made of pure magnetic materials, instead of a mixture with other constituent materials for robustness. This resulted in deviated ϵ_r and μ_r responses and evidenced the reason that the BaFe floppy disk (Fig. 7) did not down-shift f_r of the antenna as anticipated. Likewise, the samples did not enhance the efficiency of the antenna (Fig. 9) as initially anticipated; this is attributed to the high degrees of magnetic loss and $\epsilon_r \neq \mu_r$ which aggravated

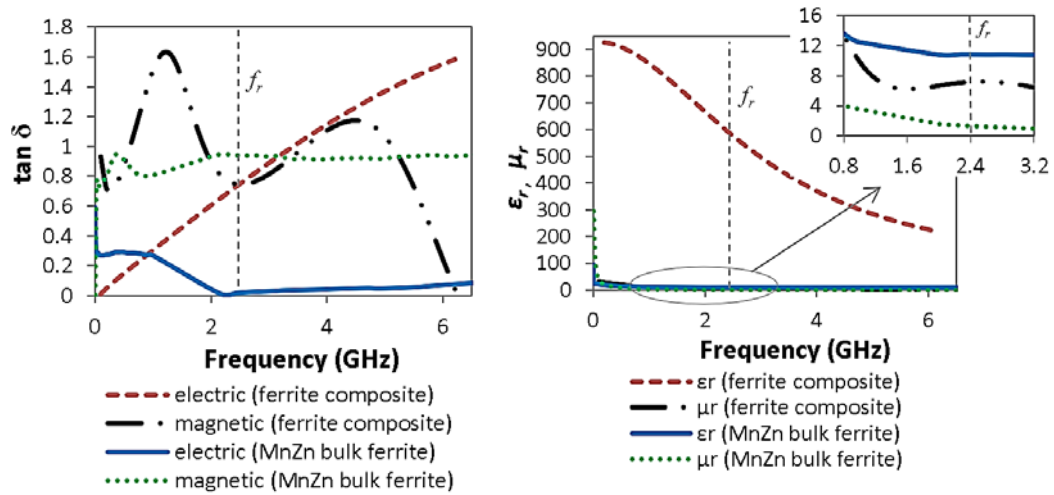


Figure 10. Measured properties of magnetic materials, ferrite composite Eccosorb NS1000Serie/MHLLSeries and MnZn bulk ferrite, as a function of frequency, (a) $\tan \delta E$, $\tan \delta M$ and (b) ϵ_r , μ_r .

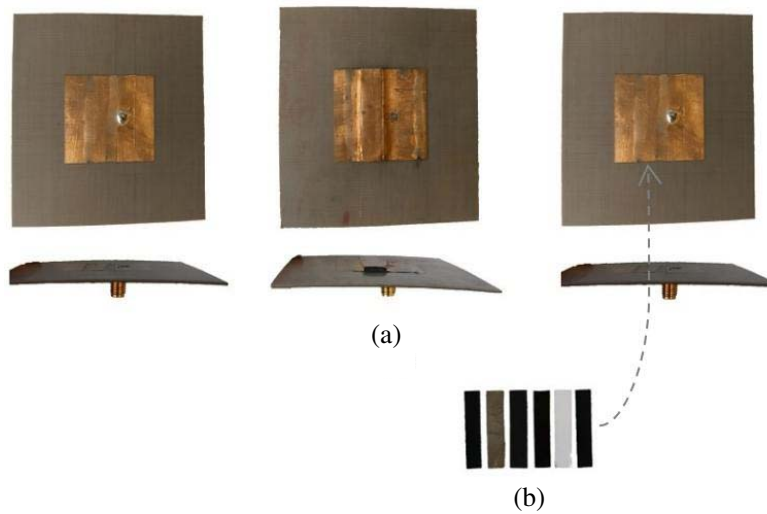


Figure 11. Fabricated antennas, (a) designs a, c and d respectively from left to right, (b) magnetic-slabs.

Table 3. Measured performance of designs a, c and e.

Design	f_r (GHz)	RL	FBW (%)	Gain (dBi)	Efficiency (%)
a	3.00	12	0.84	4.10	63.59
c	2.34	15	1.78	5.87	84.46
e	2.34	10	17.10	1.60	62.40

impedance matching control. Therefore, magnetic materials with high μ_r low ε_r (in the order of tens) and low magnetic losses are favoured in this antenna setting. The fabricated prototypes are depicted in Fig. 11.

4. CONCLUSION

A magnetic-slab located in the principal magnetic-field region beneath the patch of an antenna has been proposed. To utilise this concept effectively and avoid unnecessary use of resources, it is essential to use small quantities of magnetic materials, and thus, placing these only in certain places beneath the patch is better than making the whole substrate magnetic. For the accomplishment, a magnetic-slab embedded within the original dielectric substrate of an antenna in the prime H -field region beneath the patch reduced f_o of a conventional patch, design a, with moderate impact on its performance and is perceived as a potential to miniaturisation. However, compared to a larger volume design with a 3D dielectric ridge, design c, performance needs to be improved to be fully considered as an alternative and is conjectured to be probable using forthcoming/pending magnetic materials with improved performance by means of better sintering conditions on the power loss [19] with high saturation magnetic flux density and low power loss at high temperature [20]. The magnetic-slab antenna can benefit from mixtures/composites with a higher degree of pure magnetic material (magnetization). A magnetic-slab of material properties with high μ and low ε (in the order of tens) to improve matching control and low magnetic losses to improve efficiency is sought for future implementations. To process the proposed antenna in a practical manner, additive manufacturing, also known as 3D printing technology, can be used to model a substrate using commercially available materials. It is expected that in the near future, advances in 3D printing will develop low loss materials and be able to incorporate metallic sections for the antenna's radiator and the embedded magnetic-slab.

ACKNOWLEDGMENT

This work was supported by the EP/K011383/1 and EP/S030301/1 grants.

Thanks to Iñaki García Inal, St. George English School — Bilbao, for proofreading this manuscript. Thanks to Elijah Adegoke and Syed Bukhari, Loughborough University, for their constant support and Eva Siuda, PPG IND Inc., staff, Laird Inc., Sho Fukushima, Toda Kogyo Corp., and Carsten Dubs, Innovent, for their technical advice.

REFERENCES

1. Hansen, R. C., *Electrically Small, Superdirective and Superconducting Antennas*, Wiley, New Jersey, 2006.
2. Perruisseau-Carrier, J., M. Tamagnone, J. S. Gomez-Diaz, and E. Carrasco, "Graphene antennas: Can integration and reconfigurability compensate for the loss?" *Proceedings of the 43rd European Microwave Conference (EuMA)*, 369–372, Nuremberg, Germany, Oct. 7–10, 2013.
3. Yang, G.-M., A. Shrabstein, X. Xing, O. Obi, S. Stoute, M. Liu, J. Lou, and N. X. Sun, "Miniaturized antennas and planar bandpass filters with self-biased NiCo-ferrite films," *IEEE Transactions on Magnetics*, Vol. 45, No. 10, 4191–4194, Nov. 2009.
4. Balanis, C. A., *Antenna Theory: Analysis and Design*, 4th Edition, Wiley, Mar. 2016.
5. Niamien, C., S. Collardey, A. Sharaiha, and K. Mahdjoubi, "Compact expressions for efficiency and bandwidth of patch antennas over lossy magneto-dielectric materials," *IEEE Antennas and Wireless Propagation Letters*, Vol. 10, 63–66, 2011.
6. Whittow, W. G., "Microstrip patch antennas with 3-dimensional substrates," *Antennas and Propagation Conference (LAPC)*, 1–5, Loughborough, Nov. 12–13, 2012.
7. Mattei, J.-L., E. Le Guen, and A. Chevalier, "Dense and half-dense NiZnCo ferrite ceramics: Their respective relevance for antenna downsizing, according to their dielectric and magnetic properties at microwave frequencies," *Journal of Applied Physics*, Vol. 117, 084904, 2015.

8. Jadhav, G. B., "Investigations of properties of spinel ferrite compound doped with rare earth ions," PhD dissertation, Babasaheb Ambedkar Marathwada University, India, Dec. 5, 2013.
9. Farzami, F., K. Forooraghi, and M. Norooziarab, "Miniaturization of a microstrip antenna using a compact and thin magneto-dielectric substrate," *IEEE Antennas and Wireless Propagation Letters*, Vol. 10, 1540–1542, 2011.
10. Hwang, Y. S., K. H. Lee, Y. S. Jeon, and W. M. Sung, "The design of a near-field antenna with a ferrite sheet for UHF EPC applications," *Journal of Electromagnetic Engineering and Science*, Vol. 14, No. 3, 317–319, 2014.
11. Medeiros Gama, A. and M. Cerqueira Rezende, "Complex permeability and permittivity variation of radar absorbing materials based on MnZn ferrite in microwave frequencies," *Materials Research*, Vol. 16, No. 5, São Carlos, Sept./Oct. 2013.
12. Zhang, Q., Z. Chen, Y. Gao, C. Parini, and Z. Ying, "Miniaturized antenna array with Co₂Z hexaferrite substrate for massive MIMO," *2014 IEEE Antennas and Propagation Society International Symposium (APSURSI)*, 1803–1804, Jul. 6–11, 2014.
13. Yang, G.-M., X. Xing, A. Daigle, O. Obi, M. Liu, L. Jing, S. Stoute, K. Naishadham, and N. X. Sun, "Planar annular ring antennas with multilayer self-biased NiCo-ferrite films loading," *IEEE Transactions on Antennas and Propagation*, Vol. 58, No. 3, 648–655, Mar. 2010.
14. Schaubert, D. H., D. M. Pozar, and A. Adrian, "Effect of microstrip antenna substrate thickness and permittivity: comparison of theories with experiment," *IEEE Transactions on Antennas and Propagation*, Vol. 37, No. 6, 677–682, Jun. 1989.
15. Poddar, D. R., J. S. Chatterjee, and S. R. Chowdhury, "On some broad-band microstrip resonators," *IEEE Transactions on Antennas and Propagation*, Vol. 31, No. 1, 193–194, Jan. 1983.
16. Hansen, R. C. and M. Burke, "Antennas with magneto-dielectrics," *Microw. Opt. Technol. Lett.*, Vol. 26, No. 2, 75–78, Jul. 2000.
17. Patel, S. S., I. J. Garcia Zuazola, and W. G. Whittow, "Antenna with three dimensional 3D printed substrates," *Microwave and Optical Technology Letters*, Vol. 58, No. 4, 741–744, Apr. 2016.
18. Motevasselian, A. and W. G. Whittow, "Patch size reduction of rectangular microstrip antennas by means of a cuboid ridge," *IET Microwaves, Antennas & Propagation*, Vol. 9, No. 15, 1727–1732, Sep. 2015.
19. Han, Y., J. Suh, M. Shin, and S. Han, "The effect of sintering conditions on the power loss characteristics of Mn-Zn ferrites for high frequency applications," *Journal de Physique IV Colloque*, Vol. 7, No. 1, C1-111–C1-112, 1997, DOI: 10.1051/jp4:1997133.
20. Xing, B. B., et al., "Mn-Zn ferrite TP4K material with low power loss at high temperature," *Applied Mechanics and Materials*, Vol. 320, 119–122, Trans Tech Publications, Ltd., May 2013.